Journal Pre-proofs

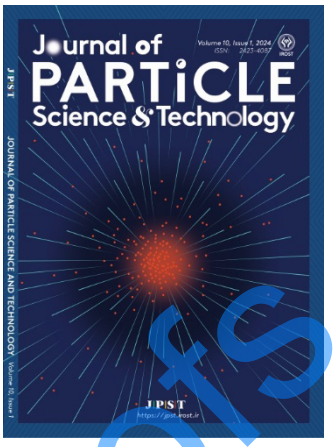

Optimization of induced gas flotation parameters for removal efficiency of near-water-density oils using response surface methodology

Sajad Bahador, Abdolreza Samimi, Davod Mohebbi-Kalhori

DOI: https://doi.org/10.22104/jpst.2025.7531.1274
Manuscript number: JPST-2504-1274

To appear in: *Journal of Particle Science and Technology (JPST)*

Received Date: 3 April 2025
Received Date in revised form: 17 October 2025
Accepted Date: 28 October 2025

Please cite this article as: Bahador S., Samimi A., Mohebbi-Kalhori D., Optimization of induced gas flotation parameters for removal efficiency of near-water-density oils using response surface methodology, *Journal of Particle Science and Technology* (2025), doi: https://doi.org/10.22104/jpst.2025.7531.1274

Optimization of Induced Gas Flotation Parameters for Removal efficiency of Near-Water-Density Oils Using Response Surface Methodology

Sajad Bahador, Abdolreza Samimi*, Davod Mohebbi-Kalhori

Department of Chemical Engineering, Faculty of Engineering, University of Sistan and Baluchestan, Zahedan, Iran

Abstract

Induced gas flotation (IGF) is an efficient physical method for separating dispersed oil from produced water. This study optimized IGF parameters for oils with near-water density (specific gravity ≈ 0.9) using Response Surface Methodology (RSM). Experiments evaluated flotation time, air-flow rate, salinity, oil concentration, and temperature. Oil-separation efficiency, defined as the percentage ratio of recovered oil mass to the initial oil mass, was measured in a 2 L glass column equipped with a silicone-membrane bubbler. The RSM model identified flotation time and salinity as dominant factors ($p < 0.05$). Optimum conditions (45 min, 0.5 L min^{-1} air flow, 20 g L^{-1} salinity, 1000 ppm oil, 20 °C) yielded about 70 % removal efficiency. Higher temperature reduced efficiency due to increased oil solubility. The results confirm IGF's applicability for challenging near-density oil systems and provide an experimentally validated optimization framework.

Keywords: Induced gas flotation; Dispersed oil; Oil-water separation; Salinity; Response Surface Methodology.

1. Introduction

Oil production generates large volumes of "produced water" that require treatment before discharge or reuse [1-8]. Purifying produced water is critical due to stringent environmental regulations [9-11]. The treatment of produced water generally involves three stages [12]. The primary physical treatment which includes sedimentation of solid particles, coalescence of free oil droplets, and their flotation. Secondary purification is applied, by using equipment such as hydrocyclones, flotation, and centrifuge units, to minimize contained oil in produced water. Tertiary treatment is employed to achieve the lowest pollution levels, using biological and physical methods such as microorganisms, activated carbon, and membrane treatments. The choice of methods for separating oil droplets from water depends on the quality standards of treated water, as well as the characteristics of the oil, gas, and water.

Flotation methods, as a secondary approach, are suitable for further treating the produced water after sedimentation [13]. These methods include electric flotation [14, 15], dissolved air flotation [16, 17], and induction gas flotation (IGF). IGF is a physical process for separating suspended substances, where induced bubbles (mainly air) are dispersed in oily wastewater. This method differs from the previous two in the way bubbles are formed. IGF involves four stages: production of fine bubbles mechanically or hydraulically, attachment of bubbles to oil drops, formation of coalesced bubbles and oil, and rising of the masses to the water surface due to buoyancy forces [18-20].

The success of the IGF process depends on the properties of water and oil (e.g., density, surface tension, contact angle, viscosity, salinity, pH, concentration, and size distribution of dispersed oil), solids (in some cases), as well as gas type [21- 23].

Oils with lower density than water can rise to the surface more quickly. However, when the densities of oil and water become quite similar, the greater size ratio of bubble to oil droplet may lead to rising of the attached oils to bubbles efficiently due to the buoyancy effect [24].

To successfully separate oil from water using IGF, the oil must first create an interface between the water and gas. Therefore, it is also crucial to consider factors that reduce the surface tension between gas and oil while increasing it between water and oil [25]. Surface tension is a fluid property that can be modified by adjusting operating conditions such as temperature, pH, bubble size distribution, water salinity, and addition of surfactants [26, 27]. Furthermore, the surface charges and forces can increase the tendency for tight junctions to form between bubbles and oil droplets [28]. In this regard, dissolved mineral salts may alter the surface energy of the oil droplets, thereby strengthening the connection between the bubble and the oil, as these salts can act as a bridge to make the connection stronger and faster [29]. Although increasing the temperature decreases viscosity and density, it also lowers the surface tension between the oil and water phases, which can inadvertently increase the solubility of the organic phase in water [30].

Numerous theoretical and experimental studies have been conducted with the aim of enhancing oil separation efficiency through IGF, using the criteria mentioned above. For example, Van Le and coworkers experimentally investigated the performance of microbubbles enhanced with normal cyclone bubbles in the separation of fine oil-in-water emulsions [31]. They achieved 86% oil separation in an acidic environment. Al-Dulaimi and Al-Yaqoobi reported oil separation by IGF in acidic and alkaline environments with efficiencies of 75% and 68%, respectively, and increased efficiency up to 84% using saline water [32]. Rajak et al. studied the mechanism and kinetics of oil separation in saline water by air flotation, achieving up to 98.3% oil separation efficiency [33]. Chakibi et al. theoretically focused on the role of bubble–drop interactions and salt addition in flotation performance [34]. Chebbi et al. treated produced water using IGF and investigated the effects of ethanol and Tween 80 conditioning on the flotation of polycyclic aromatic hydrocarbons [35]. They reduced the flotation time from 30 to 20 minutes by conditioning. As an effect of surfactant, da Silva, et al., experimentally, performed batched mode oil removal from produced water by induced air flotation using a series of nonionic surfactants [36,37]. They studied the effect of

surfactant concentration on the oil removal of oilfield produced water and obtained the maximum 80% oil removal after 4 min of flotation.

Conventional flotation methods are well established for low-density oils; however, oils with densities close to that of water remain difficult to separate. Prior studies emphasize surfactant-aided or chemically enhanced IGF, but limited research addresses purely physical optimization for near-water-density oils. Given the lack of studies focusing on oil types with a density close to water, the primary objective of this study was to employ IGF at a laboratory scale to identify the physical factors that influence separation efficiency of oil with a specific gravity of approximately 0.9. This study therefore aims to quantify the effects of salinity, flotation time, gas flow rate, oil concentration, and temperature on IGF efficiency using RSM to develop a predictive and optimized model for such systems.

2. Materials and methods

2.1. Experimental Setup, material and methods

The experimental configuration is illustrated in Fig. 1. The system consists of a transparent glass flotation column (height = 50 cm; internal diameter = 7.5 cm; effective volume = 2 lit) fitted with a silicone-membrane bubbler placed 6 cm above the base. A 24 L air compressor (model SHIMGE ZB-0.1278) was used to produced fine, medium, and coarse bubbles in the bubbler under air-flow rates of 0.5, 1.0, and 1.5 $L.min^{-1}$, respectively, (measuring flow by an air flow indicator, PLATON O2 model rotameter). Bubble sizes were measured using a high-speed digital camera (1000 fps) and analyzed in ImageJ v1.54. Each condition was replicated five times with 30–40 bubbles per frame to determine the average diameter and standard deviation. The measurement uncertainty was ± 0.05 mm.

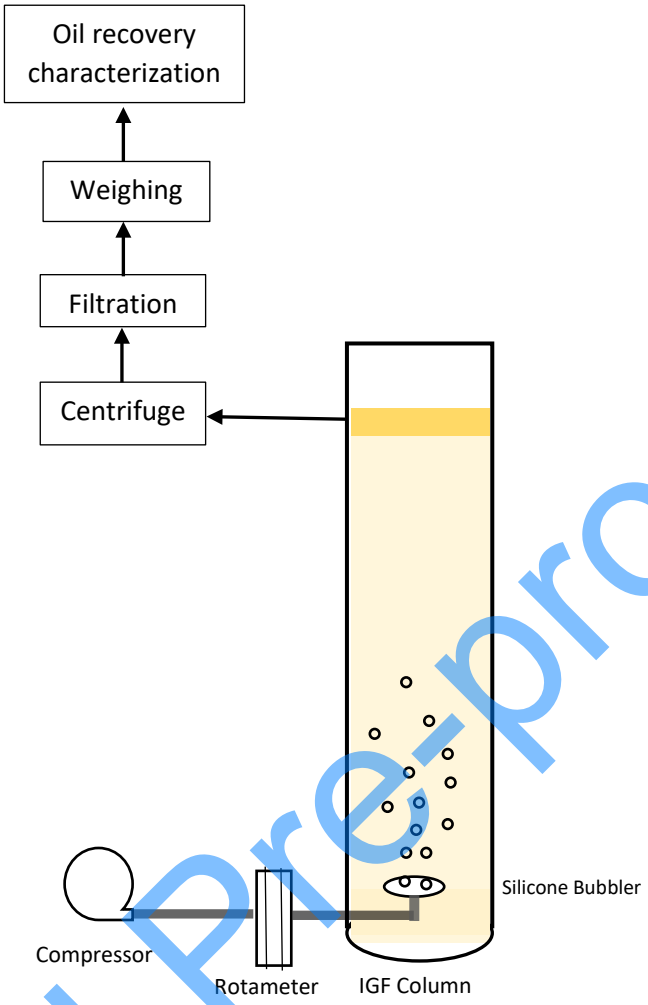

Fig. 1. Simplified schematic of the laboratory-scale Induced Gas Flotation (IGF) system showing the glass column (50 cm × 7.5 cm ID), silicone-membrane bubbler, air-compressor and flow-control system, and oil-water interface indicating bubble rise and oil removal efficiency.

Edible liquid oil, with a density of 0.9 g.mL^{-1}, was dispersed in deionized water (DW) or 10-20 g.L^{-1} NaCl saline water (SW) to prepare emulsion concentrations of 100, 550, and 1000 ppm. A high-shear mixer (model Heidolph RZR205-1) was used to make the oil-water mixture feed, rotating at 1100 rpm for 10 minutes. The droplet size of the emulsified oil was controlled primarily by the mixing rate, oil concentration, and method of oil addition. During emulsion preparation, oil was injected dropwise near the impeller tip, allowing rapid shear dispersion and preventing premature coalescence. This procedure ensured droplet uniformity across replicates and maintained consistency with the

droplet size distribution. The size distribution of the oil particles dispersed in water was observed and determined using an OLYMPUS BH-2 optical microscope and ImageJ processing software.

2.2. IGF test procedure

In each stage of the experiments, exactly 2 L of oil-water emulsion feed was transferred into the flotation column to examine the effect of various factors, including input oil concentration, water salinity, air flow rate, flotation time, and temperature. The IGF tests were carried out at both room temperature (20 °C) and 35 °C, with the suspension column heated by an external heater and the temperature measured with a mercury glass thermometer.

2.3. Oil separation efficiency

After the IGF operation completed, the oil layer floating on the water surface of the column was collected to determine the oil separation efficiency. The thin layer of oil, along with some water from the column's surface, was collected and transferred to a test tube with a lid using a pipette. The sample was then centrifuged (centrifuge model EBA 20, Germany), and the oil on the surface of the test tube was carefully separated using a syringe. The oil was transferred to a pre-weighed Whatman filter paper (2.5 µm pore size) to remove any remaining water. The oil-containing filter was kept aside at ambient temperature, and after drying for 12 hours the filter paper was weighed again using a KERN AL-J 220 balance with four decimal digits. The separation efficiency was then calculated based on the recovered and initial oil input masses using Eq. (1).

$$\eta = m_{recovered} / m_{initial} \times 100 \quad (1)$$

2.4. Statistical design and analysis

The experimental design and analysis were performed using Design-Expert v13.0 (Stat-Ease Inc., USA). A face-centered central composite design (CCD) was applied to evaluate the effects of

flotation time (30–60 min), air-flow rate (0.5–1.5 L.min^{-1}), oil concentration (100–1000 ppm), and salinity (0–20 g.L^{-1}) on oil-separation efficiency. These ranges were chosen based on preliminary screening tests that identified conditions producing measurable removal efficiency within 60 min. Model adequacy was assessed by ANOVA, coefficient of determination (R^2), adjusted R^2, predicted R^2, and lack-of-fit tests. Statistical significance was established at $p < 0.05$. In this study, the effects of parameters were investigated under ambient temperature. The parameters and levels are detailed in Table 1. It was anticipated that increasing the temperature above ambient levels would reduce the yield of oil separation. Therefore, the performance of IGF with increasing the temperature was investigated separately and it was excluded from the experiment design analysis to reduce the number of tests required.

Table 1. Factors and their level for the design of experiments with CCD face-centered method.

Symbol	Factors	Level -1	Lever +1
A	Flow rate (L min^{-1})	0.5	1.5
B	Flotation time (min)	30	60
C	Input oil concentration (ppm)	100	1000
D	Salinity of water (g.L^{-1})	0	20

3. Results and discussion

3.1. Size distribution of dispersed oil in feed water

The initial droplet size distribution of oil and its concentration are key parameters in determining the stability and characteristics of emulsions before exposure to IGF. Fig. 2 compares the count-based (number percentage) size distributions of oil droplets at different concentrations (100, 550, and 1000 ppm) dispersed in DW and SW (10 g.L^{-1}) using microscopic images, cumulative, and differential diagrams. Additionally, Table 2 presents the D50, D10, D90, and D90/D10 ratio of oil droplet sizes in SW and DW for the three concentrations, extracted from Fig. 2a–2c. The D50 represents the

median droplet size, where 50% of the droplets are larger or smaller than this value. D90 and D10 indicate the sizes over which 90% and 10% of the droplets fall, respectively. The D90/D10 ratio serves as a measure of size distribution uniformity, values closer to unity indicate a narrower distribution. As shown in Fig. 2a and Table 2, the 100 ppm oil concentration produced finer droplets, with a relatively narrower and smaller size distribution in SW compared to DW (D50 ≈ 17.5 µm in SW vs. 20.0 µm in DW; D90/D10 ≈ 0.56 in SW vs. 0.32 in DW). In contrast, the D50, D10, D90, and D90/D10 values for 550 and 1000 ppm oils showed minimal differences between SW and DW.

Furthermore, Fig. 2d–2e and Table 2 reveal that the 100 ppm concentration yielded smaller droplets (D10 ≈ 25.0 µm in SW vs. 37 µm in DW) compared to the 550 and 1000 ppm concentrations, where the size distribution extended up to 110 µm in both DW and SW (D10 ≈ 52 µm and 62 µm for 550 and 1000 ppm, respectively).

The higher oil concentrations (550 and 1000 ppm) resulted in closely packed droplets, suggesting increased droplet proximity and more frequent interactions, including coalescence. On the other hand, salinity influences interfacial tension and electrostatic repulsions, promoting the formation of smaller, more stable droplets due to a higher surface-area-to-volume ratio [26, 29]. While higher salinity favors finer droplets, increased oil concentration tends to produce larger droplets. This competition between the two effects leads to a broader size distribution at 550 and 1000 ppm compared to 100 ppm, as seen in Fig. 2a-2c.

3.2. Observation of bubbling patterns

Fig. 3 shows the bubbles rising under different incoming air flow rates (i.e., 0.5, 1.0, 1.5 L min^{-1}). The bubble sizes were measured and the approximate average sizes for small, medium, and large bubbles (Fig. 3a, 3b, and 3c) were found to be 1.10 mm, 2.25 mm, and 3.20 mm, respectively. These observations suggest the potential for coalescence into larger bubbles and their subsequent collapse

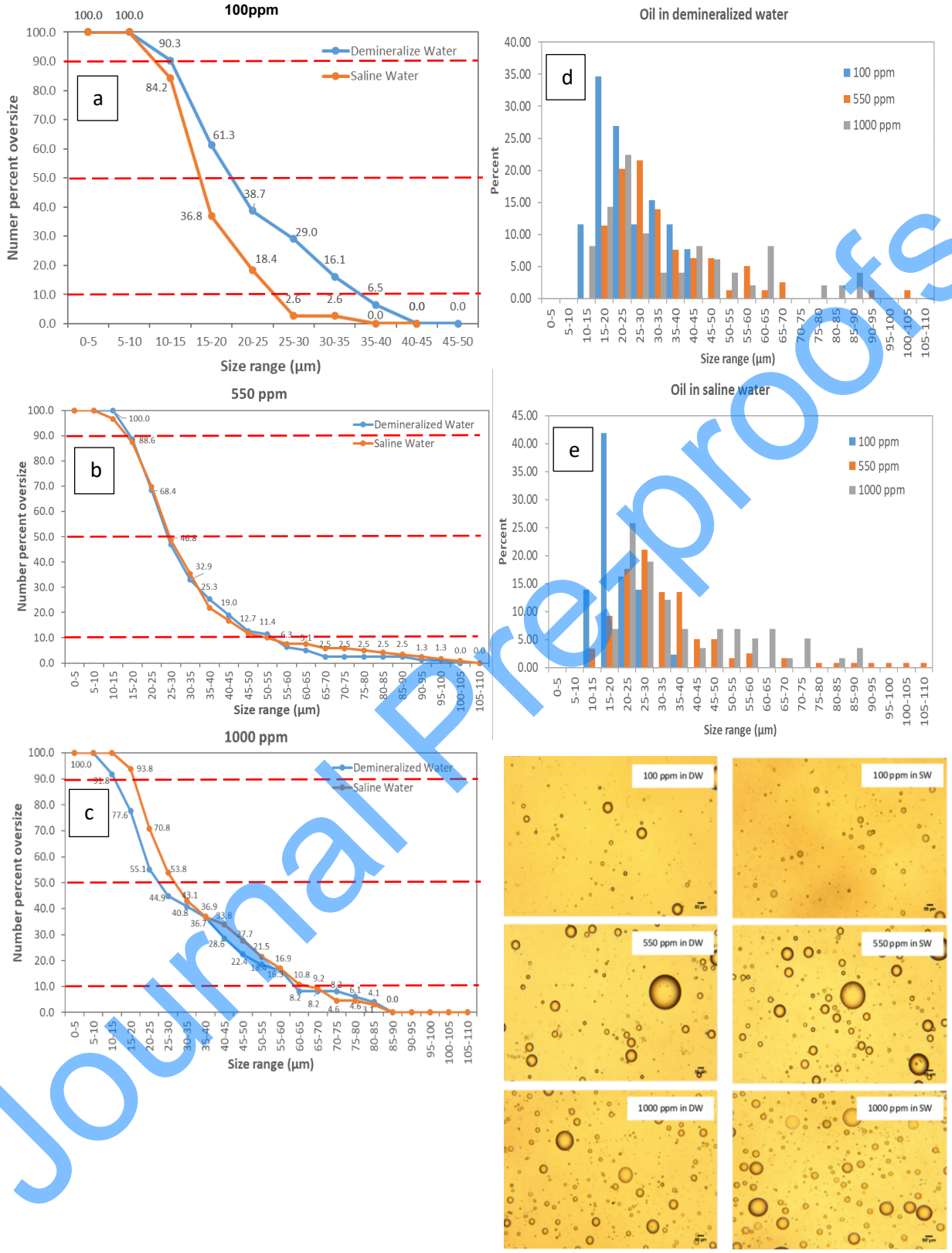

Fig. 2. Microscopic images, cumulative size distribution of oil droplets dispersed in DW and SW before IGF a) 100 ppm, b) 550 ppm, c) 1000 ppm oil, and differential size distributions of 100, 550, 1000 ppm oil d) DW and e) SW.

as they rise. At a flow rate of 1.5 L.min^{-1}, most large bubbles appeared oval, whereas at 0.5 L.min^{-1}, they were nearly spherical. By analyzing the image frames recorded by a high-speed camera at 1000 frames per second (fps), the average speed of bubbles passing by the scale bar on the flotation column was roughly calculated. Fig. 3d shows a sequence of three images of a medium-sized bubble at a flow rate of 1.0 L.min^{-1} as it ascends. Although the bubbles' paths appear spiral rather than straight, the approximate average speeds of small, medium, and large bubbles were calculated as 2.00, 2.18, and 2.30 cm.s^{-1}, respectively.

Table 2. D50, D10, D90, and D90/D10 ratio of SW and DW in 100, 550, and 1000 ppm oil concentrations.

	D50 (µm)	**D10 (µm)**	**D90 (µm)**	**D90/D10**
SW-DW (100 ppm)	17.5-20.0	25.0-37.0	14.0-12.0	0.56-0.32
SW-DW (550 ppm)	27.0-27.0	52.0-52.0	17.0-17.0	0.33-0.33
SW-DW (1000 ppm)	28.0-25.0	62.0-62.0	18.0-12.0	0.30-0.20

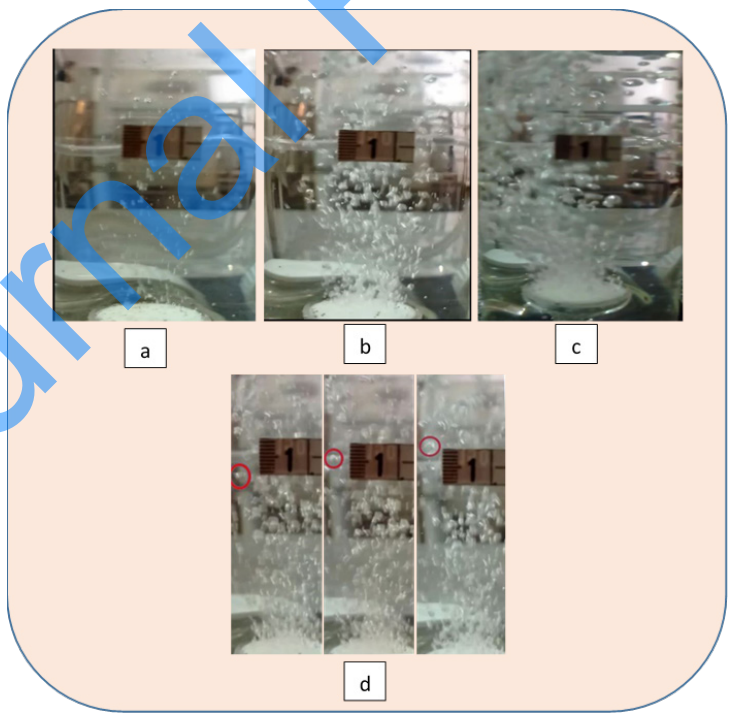

Fig. 3. Bubbling pattern images, a) small size air bubbles flow at 0.5 Lmin^{-1}, b) middle size bubbles flow at 1.0 Lmin^{-1}, c) large size bubbles flow at 1.5 Lmin^{-1}, d) high speed video images tracking of middle size bubbles.

3.3. Effect of IGF and oil concentration on separation efficiency

Fig. 4 illustrates the effect of IGF process for different oil concentrations on the percentage of oil separation, compared to non-bubbling tests in which no air induces to the column leaving the system for free flotation of dispersed oil. As seen, for all concentrations (i.e., 100, 550, 1000 ppm) dispersed in DW and at environment temperature (20 ºC), the IGF experiments cause to over 17 percent more recoveries within 60 minutes, under induced air flow rate of 0.5 L min^{-1}, compared to non-bubbling efforts at 180 minutes. It is clear that with increasing the oil concentration the operational yield also increases for both IGF and free flotation.

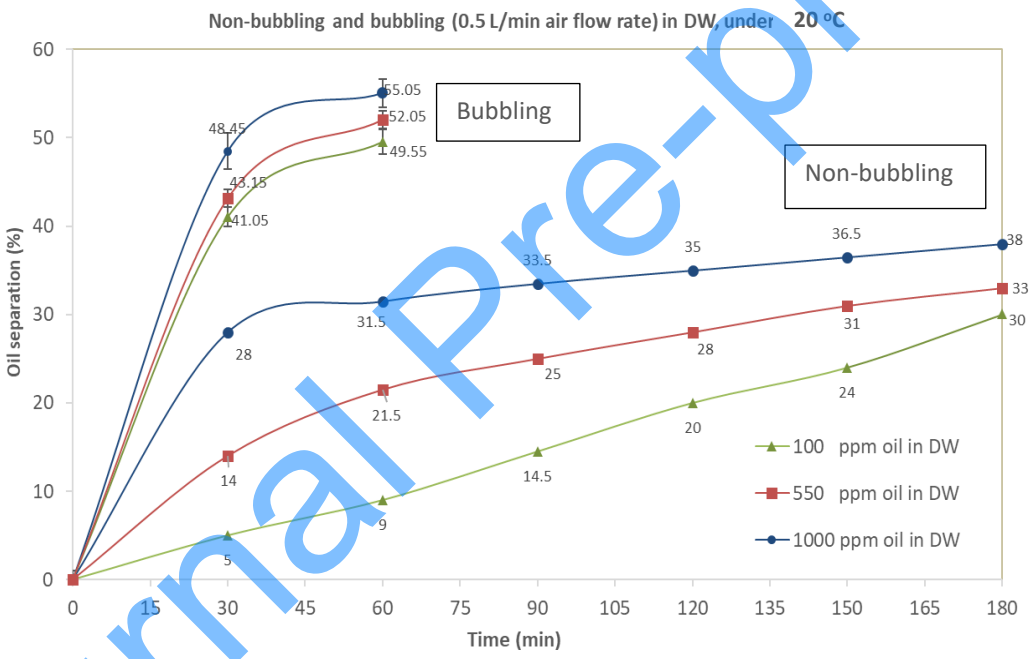

Fig. 4. Percentage of oil-separation as efficiency versus flotation time comparing non-bubbling and IGF tests for 100, 550, and 1000 ppm oil concentrations in deionized water at 20 °C.

Most of studies carried out by others often were under conditions where a significant density difference existed between the oil and water, and surfactants or coagulants were used to enhance separation efficiency [18,37]. In contrast, this study utilized an oil density of 0.9 $g.cm^{-3}$ close to water without the addition of any chemicals to the emulsion system, which presented a challenge for droplet coalescence and subsequent flotation. As a result, the maximum oil removal efficiency achieved for

free flotation system (non-bubbling) was only 38% after 180 minutes using an initial oil concentration of 1000 mg.L^{-1}. However, when the induced air was applied under 0.5 L.min^{-1}, the maximum removal efficiency increased to 55.05% for the same oil concentration and operating temperature, but within 60 minutes.

3.4. Effect of induced air flow rate, water salinity, and temperature on oil separation yield

Fig. 5 illustrates the effects of induced air flow rate, water salinity, and water temperature on the percentage of oil separation.

The percentage of oil separation versus time, comparing non-bubbling (free flotation) and bubbling (IGF under 0.5 L.min^{-1} induced gas flow rate) tests results for all concentrations (i.e., 100, 550, 1000 ppm) dispersed in DW and at environmental temperature (20 °C).

Fig. 5a shows the results of the IGF tests conducted with air flow rates of 0.5, 1.0, and 1.5 L.min^{-1} for feeds containing 1000 ppm oil dispersed in DW at a constant temperature of 20 °C. The results indicate that smaller bubbles generated at 0.5 L/min air flow yield a maximum oil separation efficiency of 55.05% after 60 minutes. In contrast, medium and large bubbles result in lower recoveries of 47.97% and 37.75% at 1.0 and 1.5 L.min^{-1}, respectively. To effectively entrain and float oil with air bubbles, it is essential for the oil droplets to form a parcially or full thin layer around the bubbles upon contact, facilitating the creation of a stable oil-gas interface [24]. Larger bubbles ascend more rapidly, while smaller bubbles, due to their increased surface area and longer retention in the column, provide better opportunities for oil droplet adhesion [18-20]. Nevertheless, in the case of bubbles much smaller than the oil droplets (e.g., micrometer-sized bubbles), they may make point contact with the oil droplets, while larger bubble in interaction with relatively smaller oil droplet is most probable to form an oil layer around the bubble [13]. Given the close densities of oil and water, the buoyancy effect for floating the oil is more efficiently achieved with a larger bubble-to-oil size ratio.

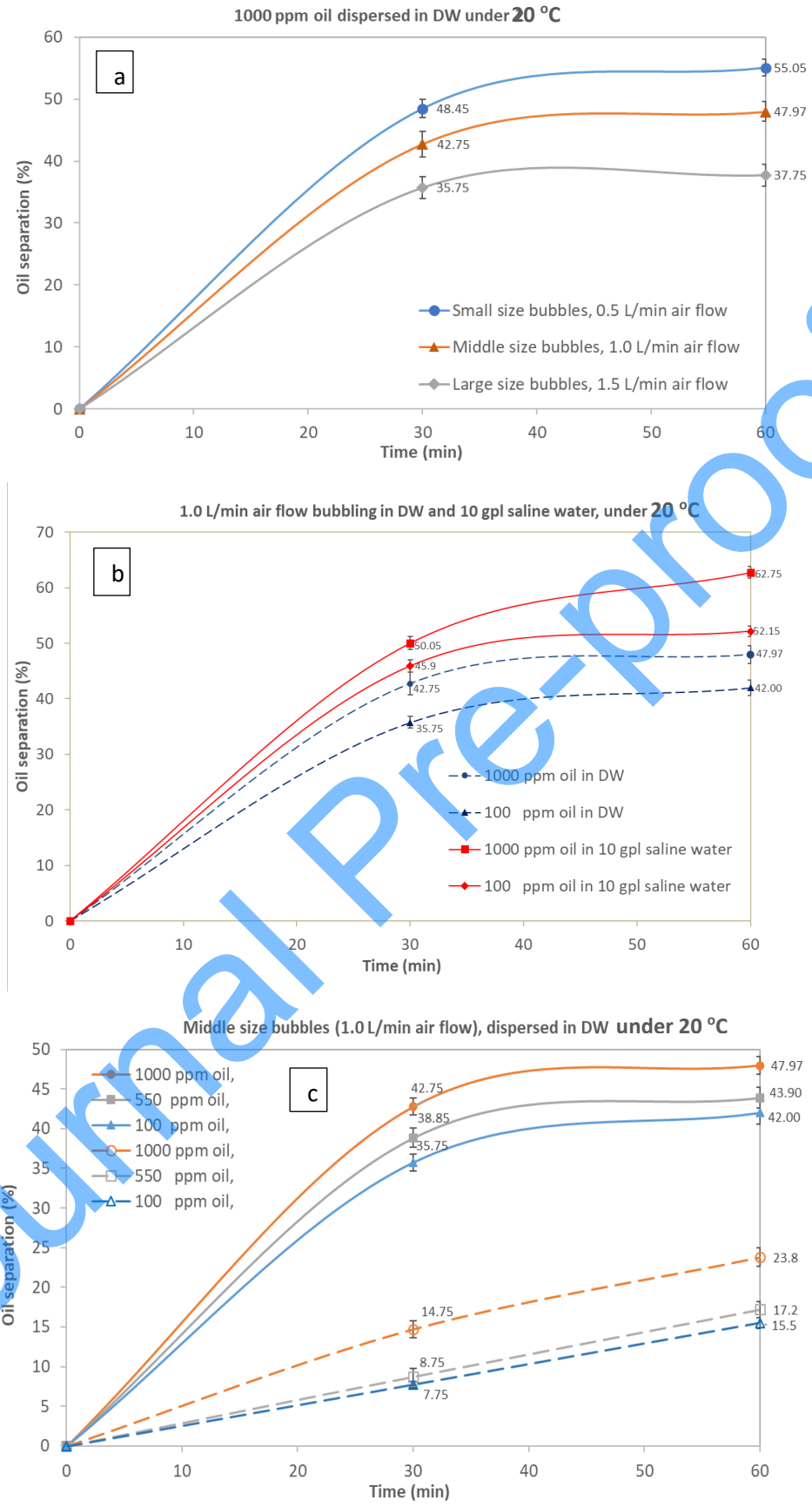

Fig. 5. Effects of (a) air-flow rate (L.min^{-1}), (b) water salinity (g.L^{-1}), and (c) temperature (°C) on oil-separation efficiency.

In the current study, the induced bubbles (approximately 1 mm in size) at a flow rate of 0.5 $L.min^{-1}$, combined with dispersed oil droplets (with a size distribution mode of 25-30 µm), create a size ratio exceeding 35, which is considered ideal. However, the optimal bubble size for a specific oil-water system is determined depending on various factors, including the column's design and operational parameters such as gas pressure and flow rates.

Fig. 5b explores the effect of water salinity (DW vs. 10 $g.L^{-1}$ NaCl) on oil separation for oil concentrations of 100 and 1000 ppm, with an air flow rate of 1.0 $L.min^{-1}$ and a water temperature of 20 °C. The results demonstrate that increasing water salinity to 10 $g.L^{-1}$ significantly enhances oil separation efficiency, reaching a maximum of 62.75% within 60 minutes for 1000 ppm oil, with similar trends observed for 100 ppm oil. These findings are consistent with previous studies, which suggest that the increased surface energy between the bubble and oil, facilitated by the presence of salt, strengthens the oil-gas interface, promoting faster and more efficient separation [26, 27, 29, 30, 32] especially in our case when the density of oil and water are close. Additionally, the reduction in bubble size with increased salinity further contributes to improved separation efficiency [26].

As the oil droplets in the continuous phase vary in size, this can influence their stability. To prevent repulsion between small oil droplets, due to their negative surface charge, this charge must be neutralized for better coalescence of droplets [16]. This can be achieved by adjusting the pH close to the isoelectric point (IEP) of the oil droplets. Surface-active agents can significantly reduce the stability of fine oil droplets, promoting the formation of larger coalesced droplets, which enhances the flotation performance [26, 27].

Fig. 5c illustrates the pronounced effect of temperature on the percentage of oil separation. A temperature increase from 20 °C to 35 °C results in approximately a 24% reduction in oil separation efficiency for 1.0 $L.min^{-1}$ air flow and 1000 ppm oil/DW. Similar reductions (about 27%) are observed for oil concentrations of 550 and 100 ppm in DW. Higher temperatures decrease the viscosity and density of the oil and water phases, as well as the interfacial tension, which can

inadvertently increase the solubility of the organic phase in water [30]. This effect is particularly significant in cases where the densities of oil and water are close, like our situation in this study.

3.5. Design of experiments and statistical analysis results using RSM

Table 3 presents the designed experiments using Design-Expert software and the Response Surface Methodology (RSM). Furthermore, Table 4 provides the analysis of variance (ANOVA) for oil separation efficiency by induced air flotation. Using ANOVA results, the prediction of fitted model were analyzed by evaluating the significance of modeling, the influence of each factor, and the its terms. As shown in Table 5, the p-values for several specified parameters are less than 0.05, indicating that these parameters have a statistically significant effect on the response with 95% confidence. The model's *F*-value was greater than 1, where a higher *F*-value indicates greater statistical significance of a term within the model. As shown in Table 5, both the coefficient of determination (R^2) and adjusted R^2 values are high enough, demonstrating that the model exhibits decent reliability.

Although the lack-of-fit test in Table 4 was statistically significant (p = 0.0134), the high R^2 (0.93) and close agreement between predicted and experimental values indicate that the model adequately represents the system. The significance likely arises from random experimental noise and unmodeled minor effects (e.g., temperature fluctuations). Given the small residual variance and acceptable predictive precision (Adeq. Precision = 20.09), the developed model is retained as valid for process optimization. As a result, the statistical valid model are obtained as Eq. (2).

$$\textit{Oil-separation efficiency (\%)} = +56.34 + 4.43A + 3.20B + 4.52C + 7.06D + 1.83AD + 1.84BC + 2.33CD - 4.49A^2 - 5.81B^2 - 5.91C^2 \quad (2)$$

where A = air-flow rate ($L.min^{-1}$), B = flotation time (min), C = oil concentration (ppm), and D = salinity ($g.L^{-1}$). All coefficients are shown with their algebraic signs, and second-order terms indicate diminishing returns beyond optimal levels.

Table 3. The designed experiments results, using Design-Expert software.

Run	Factor 1	Factor 2	Factor 3	Factor 4	Response
	A: air flow (L/min)	B: time (min)	C: input oil (ppm)	D: Salt (gr)	Oil removal efficiency (%)
1	1.0	45	550	10	53.2
2	1.5	60	1000	0	38.0
3	1.0	30	550	10	50.2
4	0.5	60	100	0	49.5
5	1.5	45	550	10	58.4
6	1.5	60	1000	20	59.3
7	0.5	60	1000	20	66.1
8	0.5	60	1000	0	55.0
9	1.5	30	1000	20	57.5
10	1.5	30	1000	0	36.2
11	1.0	45	550	10	56.4
12	0.5	60	100	20	58.6
13	1.0	45	550	20	64.7
14	1.0	45	550	10	53.3
15	1.0	45	550	10	55.1
16	0.5	45	550	10	68.5
17	1.0	45	100	10	51.2
18	1.0	45	1000	10	61.5
19	0.5	30	100	0	41.0
20	0.5	30	1000	20	65.2
21	1.5	30	100	20	44.6
22	1.0	45	550	10	54.3
23	1.0	45	550	0	41.4
24	0.5	30	1000	0	48.4
25	1.5	60	100	0	40.0
26	0.5	30	100	20	41.2
27	1.5	30	100	0	30.2
28	1.0	45	550	10	55.2
29	1.5	60	100	20	49.5
30	1.0	60	550	10	56.1

Table 4. The analysis of variance (ANOVA) for oil removal efficiency by induced air flotation.

Source	Sum of Squares	df	Mean Square	F-Value	P- Value	
Model	2447.70	10	2447.70	24.53	<0.0001	Significant
A	353.78	1	353.78	35.45	<0.0001	
B	184.32	1	184.32	18.47	0.0004	
C	368.11	1	368.11	36.88	<0.0001	
D	896.06	1	896.06	89.79	<0.0001	
AD	53.66	1	53.66	5.38	0.0317	
BC	54.39	1	54.39	5.45	0.0307	
CD	86.96	1	86.96	8.71	0.0082	
A^2	57.14	1	57.14	5.73	0.0273	
B^2	95.94	1	95.94	9.61	0.0059	
C^2	99.27	1	99.27	9.95	0.0052	
Residual	189.62	19	9.98	-	-	
Lack of fit	182.03	14	13.00	8.57	0.0134	Significant
pure error	7.59	5	1.52			

Table 5. Statistical validity of the model and input data.

Std. Dev.	3.16	**R^2**	0.9281
Mean	51.99	**Adj. R^2**	0.8903
C.V. %	6.08	**Pre. R^2**	0.7816
		Adeq. Precision	20.0855

The ANOVA results (Table 4) revealed significant interactions between air flow rate (A) and salinity (D), and between flotation time (B) and concentration (C) ($p < 0.05$). Mechanistically, the A–D interaction suggests that moderate gas flow enhances bubble–droplet collision frequency, while salinity stabilizes bubble–oil adhesion by reducing surface charge repulsion. Conversely, the B–C interaction indicates that higher oil concentrations amplify the effect of flotation time, as more

droplets become available for coalescence and attachment within the same residence period. These findings highlight that efficiency improvements result not only from physical hydrodynamics but also from interfacial charge modification due to dissolved salts.

The 3D surface plots presented in Fig. 6 illustrate the effect of air flow rate, processing time, salt concentration, and input oil concentration on the percent of oil separation efficiency.

Fig. 6a shows how oil separation efficiency changes with interaction of air flow rate (A) and retention time (B). The response surface suggests that the lowest tested air flow rates (i.e., 0.5 $L.min^{-1}$) contribute positively to oil separation efficiency, but after a certain limit time, the efficiency stabilizes or slightly declines. Time also plays a crucial role, as prolonged durations appear to increase oil separation efficiency to an optimal point (i.e., 45 minutes) before showing diminishing returns. Fig. 6b examines the influence of air flow rate (A) and salt concentration (D). The result suggests the maximum oil separation efficiency at 0.5 $L.min^{-1}$ and the highest salt concentration 20 $g.L^{-1}$. This proposes that excessive salt content (i.e., 1000 ppm) may affect the flotation or separation process positively by increasing efficiency. The relationship between time (B) and input oil concentration (C) is depicted in Fig. 6c. The trend shows that oil separation efficiency increases with time but reaches a maximum after 45 minutes. Higher input oil concentrations also contribute positively to efficiency, suggesting that more oil in the feed provides more material for separation, enhancing the efficiency. Fig. 6d analyzes the combined effects of salt concentration (D) and input oil concentration (C). The results suggest that oil separation efficiency improves with higher input oil concentrations salt levels. The positive impact of salt concentration implies that salinity might affect the stability of emulsions, by increasing coalescence of oil droplets and the efficiency of oil separation. These 3D surface plots effectively illustrate the complex interactions between different parameters influencing oil separation efficiency. Optimizing air flow, processing time, and oil concentration while maximizing salt effects and minimizing the air flowrate can lead to improved oil separation efficiency rates.

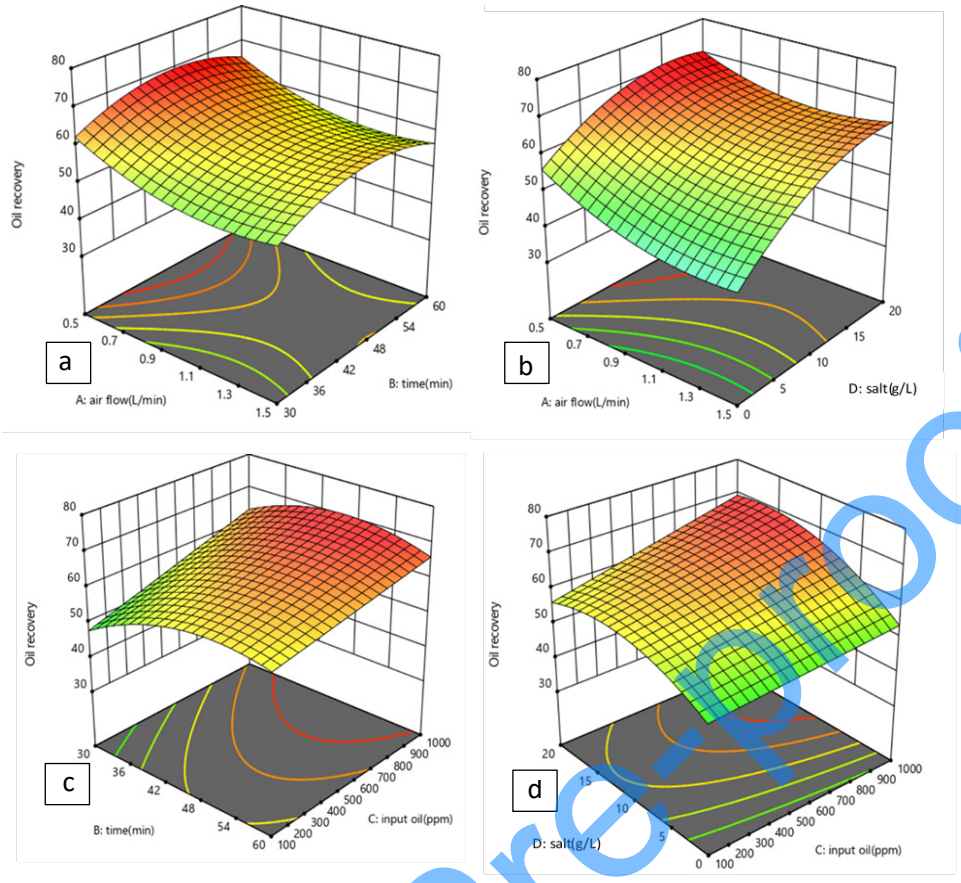

Fig. 6. 3D surface plots illustrating the effect of air flow rate, processing time, salt concentration, and input oil concentration on the percent of oil separation efficiency.

4. Conclusion

This study optimized the parameters of induced gas flotation (IGF) for separating near-water-density oils using Response Surface Methodology (RSM). The optimized physical parameters achieved a maximum oil separation efficiency of approximately 70% under the following conditions: flotation time = 45 min, air-flow rate = 0.5 L.min^{-1}, salinity = 20 g.L^{-1}, oil concentration = 1000 ppm, and temperature = 20 °C. Salinity and flotation time were identified as the dominant factors, while elevated temperature negatively influenced performance. The study confirms that fine bubbles, moderate salinity, and controlled flotation duration enhance oil–bubble adhesion and coalescence, enabling effective treatment without chemical additives. These results demonstrate that optimized IGF can treat challenging near-density oils efficiently in secondary water-treatment stages, supporting

cost-effective produced-water management in oilfields and refineries. Despite strong predictive accuracy (R^2 = 0.93), the current model does not account for droplet–bubble charge dynamics or surfactant effects. Future studies should incorporate zeta potential measurements, bubble size distribution modeling, and scale-up tests to extend IGF applicability to broader industrial systems.

References

[1] Rahimpour, M., R., Abrishami Shirazi, N., Omidvar, B., Makarem, M., A. (2023). Crisis in oil, gas, and petrochemical industries. Elsevier Inc. https://doi.org/10.1016/C2021-0-01864-2

[2] Çakmakce, M., Kayaalp, N., Koyuncu, I., (2008). Desalination of produced water from oil production fields by membrane processes. Desalination, 222(1-3), 176-186. https://doi.org/10.1016/j.desal.2007.01.147

[3] Reynolds, R.R. and Kiker, R., D., (2003). Produced water and associated issues. Oklahoma Geological Survey, Open file report.

[4] Veil, J.A ,.et al., (2004). A white paper describing produced water from production of crude oil, natural gas, and coal bed methane. US department of energy, Argonne National Lab., IL (US).

[5] Bakke, T., Klungsøyr, J., Sanni, S. (2013). Environmental impacts of produced water and drilling waste discharges from the Norwegian offshore petroleum industry. Marine environmental research, 92, 154-169. https://doi.org/10.1016/j.marenvres.2013.09.012

[6] Dudek, M., et al. (2020). Colloid chemistry and experimental techniques for understanding fundamental behaviour of produced water in oil and gas production. Advances in colloid and interface science, 276, 102-105. https://doi.org/10.1016/j.cis.2020.102105

[7] Sirivedhin, T., McCue, J., Dallbauman, L., (2004). Reclaiming produced water for beneficial use: salt removal by electrodialysis. Journal of Membrane Science, 243(1-2), 335-343. https://doi.org/10.1016/j.memsci.2004.06.038

[8] Fakhru'l-Razi, A., et al., (2009). Review of technologies for oil and gas produced water treatment. Journal of hazardous materials, 170(2-3), 530-551. https://doi.org/10.1016/j.jhazmat.2009.05.044

[9] Igunnu, E.,T., and Chen, G., Z., (2014). Produced water treatment technologies. International Journal of Low-Carbon Technologies, 9(3), 157-177. https://doi.org/10.1093/ijlct/cts049

[10] Neff, J., Lee, K., and DeBlois, E., M., (2011). Produced water: overview of composition, fates, and effects. In book; Produced water, p. 3-54. https://doi.org/10.1007/978-1-4614-0046-2_1

[11] Mc Gowin, C., et. al. (2006). Use of Produced Water in Recirculated Cooling Systems at Power Generating Facilities. Technical Report, EPRI, Palo Alto, CA and USDOE, Morgantown, WV:2006.1016458.

[12] Al-Ghouti, M., A., Al-Kaabi, M., A., Ashfaq, M., Y., Da'na, D., A., (2019). Produced water characteristics, treatment and reuse: A review. Journal of Water Process Engineering. 28, 222-239. https://doi.org/10.1016/j.jwpe.2019.02.001

[13] Saththasivam, j., Loganathan, K., Sarp, S., (2016). An overview of oil–water separation using gas flotation systems. Chemosphere. 144, 671-680. https://doi.org/10.1016/j.chemosphere.2015.08.087

[14] Hosny. A., Y., (1996). Separating oil from oil-water emulsions by electroflotation technique. Separations Technology. 6, 9-17. https://doi.org/10.1016/0956-9618(95)00136-0

[15] Abdel Khalek, M., A., et. al., (2017). Produced Water Treatment Using a New Designed Electroflotation Cell. 4, 328-338. https://doi.org/10.22105/riej.2017.100959.1022

[16] Piccioli, M., (2020). Gas Flotation of Petroleum Produced Water: A Review on Status. Fundamental Aspects, and Perspectives, Energy. 34(12) 15579–15592. https://doi.org/10.1021/acs.energyfuels.0c03262

[17] Etchepare, R., (2017). Separation of emulsified crude oil in saline water by dissolved air flotation with micro and nanobubbles. Separation and Purification Technology. 186 (2017) 326–332. http://dx.doi.org/10.1016/j.seppur.2017.06.007

[18] Wang, C., et.al. (2022). Separation of emulsified crude oil from produced water by gas flotation: A review. Science of The Total Environment. 845, 157304. https://doi.org/10.1016/j.scitotenv.2022.157304

[19] Moosai, R. and Dawe, R., A., (2003) Gas attachment of oil droplets for gas flotation for oily wastewater cleanup. Separation and purification technology, 33(3), 303-314. https://doi.org/10.1016/S1383-5866(03)00091-1

[20] Grattoni, C., Moosai, R., and Dawe, R. A., (2003). Photographic observations showing spreading and non-spreading of oil on gas bubbles of relevance to gas flotation for oily wastewater cleanup. Colloids and Surfaces A: Physicochem. Eng. Aspects 214, 151-155

[21] Moosai, R. and Dawe, R., A., (2003). Gas attachment of oil droplets for gas flotation for oily wastewater cleanup. Separation and Purification Technology. 33(3), 303-314. https://doi.org/10.1016/S1383-5866(03)00091-1

[22] Eftekhardadkhah, M., et. al., (2015). Oil Removal from Produced Water during Laboratory- and Pilot-Scale Gas Flotation: The Influence of Interfacial Adsorption and Induction Times. Energy Fuels 29(11), 7734–7740. https://doi.org/10.1021/acs.energyfuels.5b02110

[23] Painmanakul, P., et. al., (2010). Effect of bubble hydrodynamic and chemical dosage on treatment of oily wastewater by Induced Air Flotation (IAF) process. Chemical Engineering Research and Design, 88(5-6), 693-702. https://doi.org/10.1016/j.cherd.2009.10.009

[24] Naseri, A., et. al., (2015). Experimental measurement of equilibrium interfacial tension of enriched miscible gas–crude oil systems. Journal of Molecular Liquids. 211, 63-70. https://doi.org/10.1016/j.molliq.2015.05.008

[25] Rezaei, F., et.al., (2021). On the Evaluation of Interfacial Tension (IFT) of CO2–Paraffin System for Enhanced Oil Removal Efficiency Process: Comparison of Empirical Correlations, Soft Computing Approaches, and Parachor Model. Energies 2021, 14(11), 3045. https://doi.org/10.3390/en14113045

[26] Eftekhardadkhah, M., and Øye, G., (2013). Induction and Coverage Times for Crude Oil Droplets Spreading on Air Bubbles. Environ. Sci. Technol. 47(24), 14154–14160. https://doi.org/10.1021/es403574g

[27] Nenningsland, A., L., Simon, S., Sjöblom, J., (2014). Influence of Interfacial Rheological Properties on Stability of Asphaltene-Stabilized Emulsions. 35(2), 231-243. https://doi.org/10.1080/01932691.2013.784196

[28] Bertheussen, A., Simon, S., Sjöblom, J., (2017). Equilibrium partitioning of naphthenic acids and bases and their consequences on interfacial properties. Colloids and Surfaces A: Physicochemical and Engineering Aspects. 529, 45-56. https://doi.org/10.1016/j.colsurfa.2017.05.068

[29] Fanaie, V.R., and Khiadani, M., (2020). Effect of salinity on air dissolution, size distribution of microbubbles, and hydrodynamics of a dissolved air flotation (DAF) system. Colloids and Surfaces A: Physicochemical and Engineering Aspects. 591,124547. https://doi.org/10.1016/j.colsurfa.2020.124547

[30] Chiesa, M., et. al., (2008). Thermal conductivity and viscosity of water-in-oil nanoemulsions. Colloids and Surfaces A: Physicochemical and Engineering Aspects. 326(1-2), 67-72. https://doi.org/10.1016/j.colsurfa.2008.05.028

[31] Van Le, T., et al., (2013) Performance of tiny microbubbles enhanced with "normal cyclone bubbles" in separation of fine oil-in-water emulsions. Chemical Engineering Science, 94, 1-6. http://dx.doi.org/10.1016/j.ces.2013.02.044

[32] Al-Dulaimi, S.L. and Al-Yaqoobi, A., M., (2021). Separation of oil/water emulsions by microbubble air flotation. in IOP Conference Series: Materials Science and Engineering. IOP Publishing. https://doi.org/10.1088/1757-899X/1076/1/012030

[33] Rajak, V., et al., (2015). Mechanism and kinetics of separation of oil from oil-in-water emulsion by air flotation. Petroleum Science and Technology. 33(23-24), 1861-1868. https://doi.org/10.1080/10916466.2015.1108987

[34] Chakibi, H., et al., (2018). Role of bubble–drop interactions and salt addition in flotation performance. Energy & Fuels, 32(3), 4049-4056. https://doi.org/10.1021/acs.energyfuels.7b04053

[35] Chebbi, S., et al., (2019). Treating Produced Water Using Induced Air Flotation: The Effect of Ethanol on Conditioning and Flotation of PAHs in the Presence of Tween 80. Polish Journal of Environmental Studies. 28(4). DOI: https://doi.org/10.15244/pjoes/89985

[36] da Silva, S.S., et al., (2015). Oil removal of oilfield-produced water by induced air flotation using nonionic surfactants. Desalination and Water Treatment, 56(7), 1802-1808. https://doi.org/10.1080/19443994.2014.958103

[37] Shen, W., (2022). Microbubble and nanobubble-based gas flotation for oily wastewater treatment: a review. Environ. Rev. 30, 359–379. https://doi.org/10.1139/er-2021-0127